Components of TOR and MAP kinase signaling control chemotropism and pathogenicity in a fungal pathogen

Vasileios Vangalis[a], Emmanouil A. Markakis[b], Michael Knop[c,d], Antonio Di Pietro[e], Milton A. Typas[a,*], Ioannis A. Papaioannou[c,*]

[a] Department of Genetics & Biotechnology, Faculty of Biology, National and Kapodistrian University of Athens, 15784, Athens, Greece

[b] Laboratory of Mycology, Department of Viticulture, Vegetable Crops, Floriculture and Plant Protection, Institute of Olive Tree, Subtropical Crops and Viticulture, N.AG.RE.F., Hellenic Agricultural Organization - DIMITRA, 71307, Heraklion, Crete, Greece

[c] Center for Molecular Biology of Heidelberg University (ZMBH), 69120, Heidelberg, Germany

[d] German Cancer Research Center (DKFZ), DKFZ-ZMBH Alliance, 69120, Heidelberg, Germany

[e] Departamento de Genética, Campus de Excelencia Internacional Agroalimentario ceiA3, Universidad de Córdoba, 14014, Córdoba, Spain

[*] Corresponding authors.

Email addresses:

vasvagg@biol.uoa.gr (Vasileios Vangalis); markakis@elgo.iosv.gr (Emmanouil A. Markakis); m.knop@zmbh.uni-heidelberg.de (Michael Knop); ge2dipia@uco.es (Antonio Di Pietro); matypas@biol.uoa.gr (Milton A. Typas); i.papaioannou@zmbh.uni-heidelberg.de (Ioannis A. Papaioannou)

ORCID IDs:

Vasileios Vangalis: 0000-0002-6501-7052

Emmanouil A. Markakis: 0000-0002-8791-0669

Michael Knop: 0000-0003-2566-923X

Antonio Di Pietro: 0000-0001-5930-5763

Ioannis A. Papaioannou: 0000-0002-8055-4024

ABSTRACT

Filamentous fungi can sense useful resources and hazards in their environment and direct growth of their hyphae accordingly. Chemotropism ensures access to nutrients, contact with other individuals (e.g., for mating), and interaction with hosts in the case of pathogens. Previous studies have revealed a complex chemotropic sensing landscape during host-pathogen interactions, but the underlying molecular machinery remains poorly characterized. Here we studied mechanisms controlling directed hyphal growth of the important plant pathogenic fungus *Verticillium dahliae* towards different chemoattractants. We found that the homologs of the Rag GTPase Gtr1 and the GAP (GTPase-Activating Protein) Tsc2, an activator and a repressor of the TOR kinase respectively, which have not been analyzed in filamentous fungi before, play important roles in hyphal chemotropism towards nutrients, plant-derived signals, and synthetic α-pheromone from the plant pathogenic fungus *Fusarium oxysporum*. Furthermore, important roles of these regulators were identified in fungal development and pathogenicity. We also included in our study components of mitogen-activated protein kinase (MAPK) cascades and found that the MAPK Fus3 is required for chemotropism towards nutrients, while the G protein-coupled receptor (GPCR) Ste2 and MAPK Slt2 control chemosensing of plant-derived signals and α-pheromone. Our study establishes *V. dahliae* as a suitable model for the analysis of fungal chemotropism and discovers new components and mechanisms of chemotropic signaling, such as the TOR pathway, during growth and host-pathogen interactions of *V. dahliae*.

Keywords

autophagy, chemotropism, environmental sensing, mTOR signaling pathway, pathogenicity, *Verticillium dahliae*

1. Introduction

Filamentous fungi grow and colonize their substrates by polarized tip extension and lateral branching of their hyphae (Riquelme, 2013). Since the necessary resources for their survival are heterogeneously distributed in their habitats, fungi have evolved mechanisms for sensing the environment and responding by directed growth (Brand and Gow, 2009; Leeder et al., 2011). This results from dynamic re-orientation of hyphal growth towards or away from stimuli such as nutrients, toxic substances, other individuals (e.g., during mating and vegetative fusion), and host organisms (Lombardi et al., 2018; Moreno-Ruiz et al., 2020; Sridhar et al., 2020; Turrà et al., 2015; Vangalis et al., 2021a). In the case of fungal pathogens, chemotropic sensing and growth play prominent roles during host-pathogen interactions (Turrà et al., 2016). However, the underlying mechanisms of sensing and processing chemotropic signals are still not fully understood (Turrà et al., 2016; Van Dijck et al., 2017).

Various classes of membrane proteins such as non-transporting receptors, transceptors, and G protein-coupled receptors (GPCRs) have important roles in nutrient sensing (Van Dijck et al., 2017). Studies in the plant-pathogenic ascomycete *Fusarium* spp. have implicated the GPCR Ste2, a homolog of the alpha-factor pheromone receptor from *Saccharomyces cerevisiae*, in chemotropic sensing of the host plant (Nordzieke et al., 2019; Sridhar et al., 2020; Turrà et al., 2015). The signal is then transduced to the mitogen-activated protein kinase (MAPK) Mpk1 (Slt2 in yeast), a component of the cell wall integrity (CWI) signaling pathway, to mediate the chemotropic response (Nordzieke et al., 2019; Sridhar et al., 2020; Turrà et al., 2015).

The CWI MAPK cascade is required for remodeling of the fungal cell wall and ensures its integrity under cell wall stress. Deletion of homologs of filamentous fungi results in defects in hyphal growth, hypersensitivity to cell wall-damaging agents, and often reduced pathogenicity against plant or animal hosts (reviewed by Zhao et al. 2007; Turrà et al. 2014; Jiang et al. 2018). Apart from its role in the chemotropic response to plant signals, Mpk1 in *F. oxysporum* has also been implicated in the response to α-pheromone as a cell density-dependent autocrine signal to control germination of conidia (Turrà et al., 2015; Vitale et al., 2019). Furthermore, the homolog of *Neurospora crassa* has been shown to participate, together with the Fus3 homolog, in an oscillatory mechanism that mediates communication of anastomosis tubes during vegetative hyphal fusion (Fischer and Glass, 2019; Fleissner et al., 2009). Moreover, in *F. oxysporum,* the MAPK homolog of Fus3 is required for the chemotropic response to different nutrients in a Ste2-independent manner (Turrà et al., 2015). In addition to these functions, Fus3 homologs play important roles in fungal development and pathogenicity (reviewed by Zhao et al. 2007; Turrà et al. 2014; Jiang et al. 2018).

In eukaryotes, Target Of Rapamycin (TOR) kinase complexes respond to multiple environmental cues (Dobrenel et al., 2016; Workman et al., 2014) to regulate cellular development, proliferation, and survival by controlling metabolic processes, nutrient uptake, autophagy, as well as protein production and degradation (Chantranupong et al., 2015; Saxton and Sabatini, 2017; Workman et al., 2014). In filamentous fungi, the TOR signaling pathway was shown to be involved in the regulation of nutrient sensing, hyphal growth and morphogenesis, cell cycle regulation, and stress response (Fitzgibbon et al., 2005; Li et al., 2019; Weisman, 2016; Yu et al., 2014). The GTPases Rag1/2 and Rheb, as well as their respective repressors GATOR1 and TSC1/2, are important regulators of the TOR kinase complex 1 (TORC1) in higher eukaryotes, and they are conserved in fungi (i.e., GTPases Gtr1/2 and Rhb1, and GAP repressors SEACIT and TSC1/2, respectively) (Wolfson and Sabatini, 2017). Characterization of the Gtr1/2 complex in *S. cerevisiae* revealed its participation in the activation machinery of TORC1 in response to amino acids or other nitrogen sources (Binda et al., 2009; Kira et al., 2016, 2014) and this was further supported by evidence from *Schizosaccharomyces pombe* (Valbuena et al., 2012). On the other hand, deletion of *tsc1* or *tsc2* in the *Sc. pombe* led to hyperactivation of TORC1 and a reduction of amino acid uptake (Matsumoto et al., 2002; Slegtenhorst et al., 2004).

The ascomycete *Verticillium dahliae* is a soilborne plant pathogen that causes economically devastating wilt disease on a wide range of commercially important plants and crops (Pegg, G.F and Brady, B.L., 2002). The infection cycle of *V. dahliae* starts with germination of microsclerotia (i.e., resting structures) induced by plant root exudates, penetration of roots by elongating hyphae, and colonization of the host's vascular system (Klosterman et al., 2009). The mechanisms used for sensing and growing towards plant-derived signals are currently unknown.

In this study, we used *V. dahliae* as a fungal model to elucidate the molecular machinery for environmental sensing and chemotropism towards nutrients and plant hosts. For this, we examined two members of the TOR signaling pathway, Gtr1 and Tsc2, that have not been studied previously in filamentous fungi, as well as the MAPKs Fus3 and Slt2 and the GPCR Ste2. Our results provide new insights into the fungal nutrient and host sensing machinery and establish *V. dahliae* as a suitable model for the analysis of MAPK and TOR signaling in fungal plant pathogens.

2. Materials and Methods

2.1. Strains and culture conditions

All *V. dahliae* strains and plasmids that were used and constructed in this study are listed in Supplementary Tables 1 and 2, respectively (Lu et al., 1994; Nguyen et al., 2008; Paz et al., 2011). Culture media and conditions, preparation, handling, and maintenance of monoconidial strains have been described previously (Papaioannou et al., 2013; Vangalis et al., 2021a).

2.2. Gene deletion and complementation of knockout strains

Deletion strains Δ*gtr1* and Δ*tsc2*, as well as double deletion strains Δ*fus3* Δ*slt2* and Δ*fus3* Δ*ste2* were constructed in this study in the background of the wild-type *V. dahliae* isolate 123V (Supplementary Table 1). For this, we used our optimized *Agrobacterium tumefaciens*-mediated transformation protocol and constructed plasmids for double homologous recombination, as previously described (Vangalis et al., 2020). All knockout mutants were validated by PCR using gene-specific primers and Southern hybridization analyses (Supplementary Fig. 1). For complementation of the knockout strains, the corresponding wild-type genes with their flanking regions were re-introduced, according to our previously reported procedures (Vangalis et al., 2020). We also included in parts of our study *V. dahliae* 123V deletion mutants Δ*fus3*, Δ*slt2*, and Δ*ste2*, which were previously reported (Vangalis et al., 2021a).

2.3. Quantitative analysis of chemotropism

Chemotropic responses were quantified using a plate assay previously employed in *Fusarium oxysporum* (Turrà et al., 2015) with minor modifications. Freshly obtained *V. dahliae* conidia were embedded in 5 mL of three times diluted Czapek-Dox Minimal Medium (MM/3) supplemented with 0.5% agar (w/v), at a final concentration of 2.5×10^6 per mL, which was poured into a Petri dish. A central scoring line was drawn on the bottom of the plate, and two parallel wells were cut into the medium on both sides, at 6 mm distance from the scoring line. Then, 50 μL of the test compound solution and of the solvent control was added to the wells at the two sides of the scoring line, respectively. Tested compounds and standard concentrations used were sodium aspartate (Asp) and methionine (Met) at 295 mM; ammonium nitrate (NH_4^+), glucose (Gluc), glycerol (Glyc), and sodium glutamate (Glu) at 100 mM; and pectin (Pec) at 1% (w/v) (all from Sigma Aldrich, Saint Louis, MO, USA). Sterile water

or methanol were used as solvent controls, as appropriate. To measure the chemotropic response towards host plants, the root of a 2-week-old tomato seedling was placed directly on one of the wells. Lyophilized peptides of synthetic *F. oxysporum* α-pheromone (Turrà et al., 2015) were dissolved in 50% (v/v) methanol in water and assayed at a concentration of 378 μM. To test the effect of different treatments on the chemoattractant activity of *F. oxysporum* α-pheromone or tomato root exudates, the peptide and the exudates were incubated for 10 min at 100 °C or treated with 1 mg/mL proteinase K (Sigma Aldrich, Saint Louis, MO, USA). Plates were incubated at 25 °C in the dark for 14 h, and chemotropism of conidial germ tubes was then recorded as described (Turrà et al., 2015) using an Olympus (Olympus Corporation, Shinjuku City, Tokyo, Japan) binocular microscope (200× magnification). The chemotropic index used to quantify chemotropism (Fig. 1A) was calculated by the formula [(germ tubes pointing the stimulus – germ tubes pointing the solvent)/(total number of germ tubes) × 100] (Turrà et al., 2015). A total of 400 hyphal tips were scored for each test compound. All experiments were performed at least twice. Statistical analysis was conducted using *t*-test.

2.4. Western blot analyses

To study MAPK phosphorylation in response to different compounds, 5×10^6 conidia per mL were allowed to germinate for 24 h in PDA medium at 25 °C and 170 rpm. Samples of fungal mycelium were collected before (time 0) and after the addition of each compound. Protein extraction was performed with a lysis buffer containing 0.2 M NaOH and 0.2% (v/v) β-mercaptoethanol, followed by precipitation with 7.5% trichloroacetic acid (TCA) (Méchin et al., 2007). Western blotting was performed as described (Segorbe et al., 2017). Protein samples were resolved in 10% SDS-polyacrylamide gels and transferred to nitrocellulose membranes using the Trans-Blot Turbo RTA Midi Nitrocellulose Transfer Kit (#1704271 from Bio-Rad Laboratories, Hercules, CA, USA). Phosphorylation of MAPKs Slt2 and Fus3 was detected using a rabbit antiPhospho-p44/42 MAPK (Erk1/2) antibody (Thr202/Tyr204; #4370 from Cell Signaling Technology, Danvers, MA, USA). A mouse anti-α-tubulin antibody (#T9026 from Sigma Aldrich, Saint Louis, MO, USA) was used for the loading controls. Visualization of the corresponding bands was performed using the ECL™ Select western blotting detection reagent (GE Healthcare, Chicago, IL, USA) in a LAS-3000 detection system (Fujifilm España, Barcelona, Spain).

2.5. Plant pathogenicity assays

Plant pathogenicity bioassays were performed according to previously published protocols (Markakis et al., 2014; Vangalis et al., 2020). Briefly, eggplant seedlings at the one true leaf stage were drenched with 20 mL of conidial suspensions (5.0×10^6 conidia per mL) or sterile water (mock infection controls). Treated plants were incubated at 25 °C with a 12-h light-dark cycle. Assessment of disease severity at each time point (up to 31 days) and determination of relative AUDPC and plant growth parameters was performed as previously described (Markakis et al., 2014; Vangalis et al., 2020). Fungal re-isolation was performed from sections along the stem of each treated plant (three chips from nine randomly selected plants per treatment) as previously described (Markakis et al., 2014). The re-isolation ratio was expressed as the number of xylem chips from each treatment that exhibited fungal growth.

2.6. Morphological characterization and stress response of V. dahliae strains

Morphological and physiological characterization of fungal strains, and assessment of their stress tolerance were performed as previously described (Vangalis et al., 2021c). All experiments were performed at least in triplicate. To determine the frequency of conidial germination, 100 conidia per strain and replicate were analyzed. Strains were exposed to a variety of oxidative agents (H_2O_2, paraquat, iprodione, farnesol), substances that induce osmotic stress (NaCl, sorbitol), cell wall damaging factors (amphotericin B obtained from Biosera, Nuaille, France; fluconazole from Pfizer, Brooklyn, NY, USA; calcofluor white M2R, Congo red), an inhibitor of TOR kinase (sirolimus from Cayman Chemical, Ann Arbor, MI, USA), and fungicides (azoxystrobin, cymoxanil). All were purchased from Sigma Aldrich (Saint Louis, MO, USA) unless otherwise indicated. For quantification of sensitivity to the tested compound, relative growth inhibition was calculated by the formula [(colony diameter on CM − colony diameter in stress condition)/(colony diameter on CM) × 100)].

3. Results

3.1. A quantitative assay for the analysis of chemotropism in V. dahliae

For the purposes of our study, we first optimized a quantitative chemosensing assay for *V. dahliae* on agar plates, based on a procedure that was previously used in *F. oxysporum* (Turrà et al., 2015). Our optimized assay (described schematically in Fig. 1A; details in paragraph 2.3) exposes *V. dahliae* germlings to gradients of diffusing substances and enables microscopic recording of the growth orientation of hyphal tips. When germlings of the wild-type strain 123V were tested against a variety of carbon and nitrogen sources, we found glucose, pectin, and the amino acids glutamate, aspartate, and methionine to induce strong positive chemotropic responses, in contrast to glycerol, galactose, and ammonium nitrate (Fig. 1B). Our further analyses of responses to glucose and glutamate revealed that hyphal chemotropism is dose-dependent, with particularly low and high concentrations both failing to induce strong reactions (Fig. 1C). Hyphal tips were significantly attracted by tomato roots, as well as by root exudates of tomato and *Arabidopsis* plants that were tested (Fig. 1D). This directed hyphal growth was largely reduced when exudates were boiled or treated with proteinase K. Although *V. dahliae* is widely regarded as an asexual fungus, it exhibited significant chemotropic responses to synthetic α-pheromone of *F. oxysporum*, which were also reduced upon treatment with proteinase K (Fig. 1D).

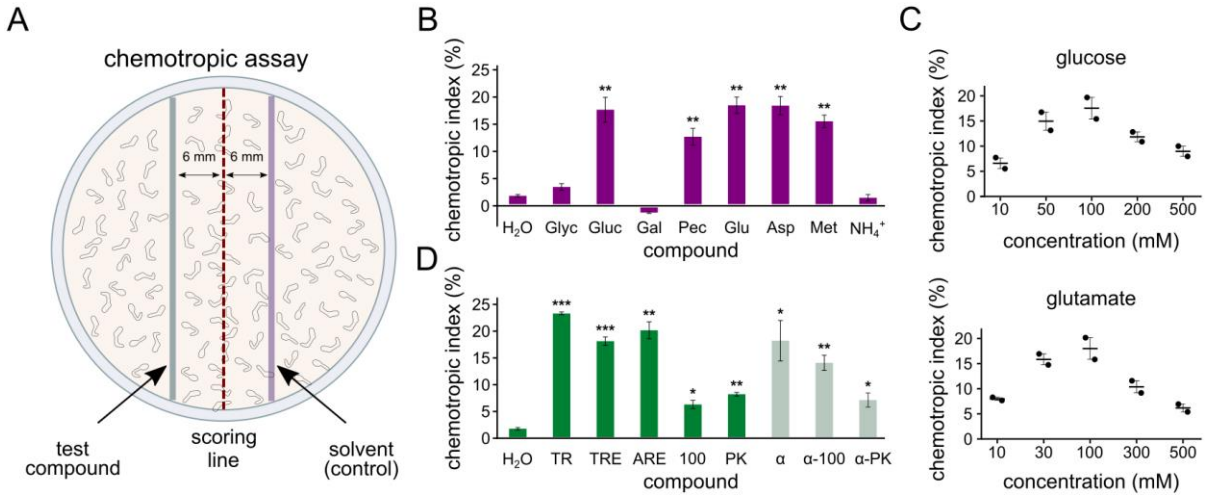

Fig. 1. Optimization of a chemotropism assay in *V. dahliae* **A.** Schematic representation of the chemotropism assay (modified from Turrà et al. 2015). **B.** Chemotropism of the wild-type strain 123V towards the nutrient sources glycerol (Glyc), glucose (Gluc), galactose (Gal), pectin (Pec), glutamate (Glu), aspartate (Asp), methionine (Met), and ammonium nitrate (NH_4^+). **C.** Dose-dependent chemotropic response to the indicated concentrations of glucose and glutamate. **D.** Chemotropism of the wild-type strain 123V towards tomato roots (TR), tomato root exudate (TRE), *Arabidopsis* root exudate (ARE), α-pheromone (α), or towards tomato root exudate or α-pheromone after boiling (100 and α-100, respectively) or treatment with proteinase K (PK and α-PK, respectively). Bars (in **B-D**): SD.

Statistical significance of differences from the control condition (H_2O) in **B** and **D** was tested with Student's *t*-test (* $p<0.05$, ** $p<0.01$, *** $p<0.001$).

3.2. Differential roles of the MAPKs Fus3 and Slt2 in chemotropism of V. dahliae towards nutrients, α-pheromone, and plant signals

The function of MAP kinase signaling cascades is known to be important for a variety of biological processes, including environmental sensing in other organisms (Zhao et al., 2007; Turrà et al., 2014, 2016). This motivated us to analyze further the *V. dahliae* homologs of MAPKs Fus3 and Slt2 in our study. Deletion of *fus3* led to markedly reduced production of microsclerotia (Fig. 2A), reduced growth, compromised sporulation (Fig. 2B), and increased sensitivity to oxidative stress (Supplementary Fig. 2). The Δ*slt2* mutant also exhibited complete inability to produce microsclerotia, drastic reduction of aerial mycelium (Fig. 2A), defective sporulation (Fig. 2B), and significant growth inhibition by chemicals that induce cell wall stress (Supplementary Fig. 2). Double deletion of *fus3* and *slt2* resulted in a Δ*fus3* Δ*slt2* mutant showing combined defects of the single mutants as well as an additional defect in conidial germination that was specific for the double mutant (Fig. 2A-B).

We used the chemotropic assay to test these deletion mutants for the ability to sense and orient their hyphal tips towards nutrients or hosts in their environment. The MAPK Fus3 was necessary for normal chemotropism towards nutrients, while Slt2 was required for chemotropism towards root exudates and synthetic *F. oxysporum* α-pheromone peptide (Fig. 2C). In line with this, the double mutant Δ*fus3* Δ*slt2* failed to respond to any of the tested stimuli (Fig. 2C). Wild-type behavior was fully rescued by complementation of our deletion mutants with the respective wild-type alleles (Fig. 2C).

We next determined the MAPK phosphorylation levels in germlings exposed for 15 min to various stimuli. Immunoblot analysis revealed a significant dephosphorylation of Slt2 upon exposure to the nutrient chemoattractants glucose and methionine, but not to root exudates (Fig. 2D). Interestingly, exposure to ammonium nitrate, a nutrient source that does not induce a chemotropic response did not alter the phosphorylation levels of Slt2 (Fig. 2D). A time-course experiment revealed that Slt2 dephosphorylation in response to glucose was already detectable 5 min upon exposure (Fig. 2E).

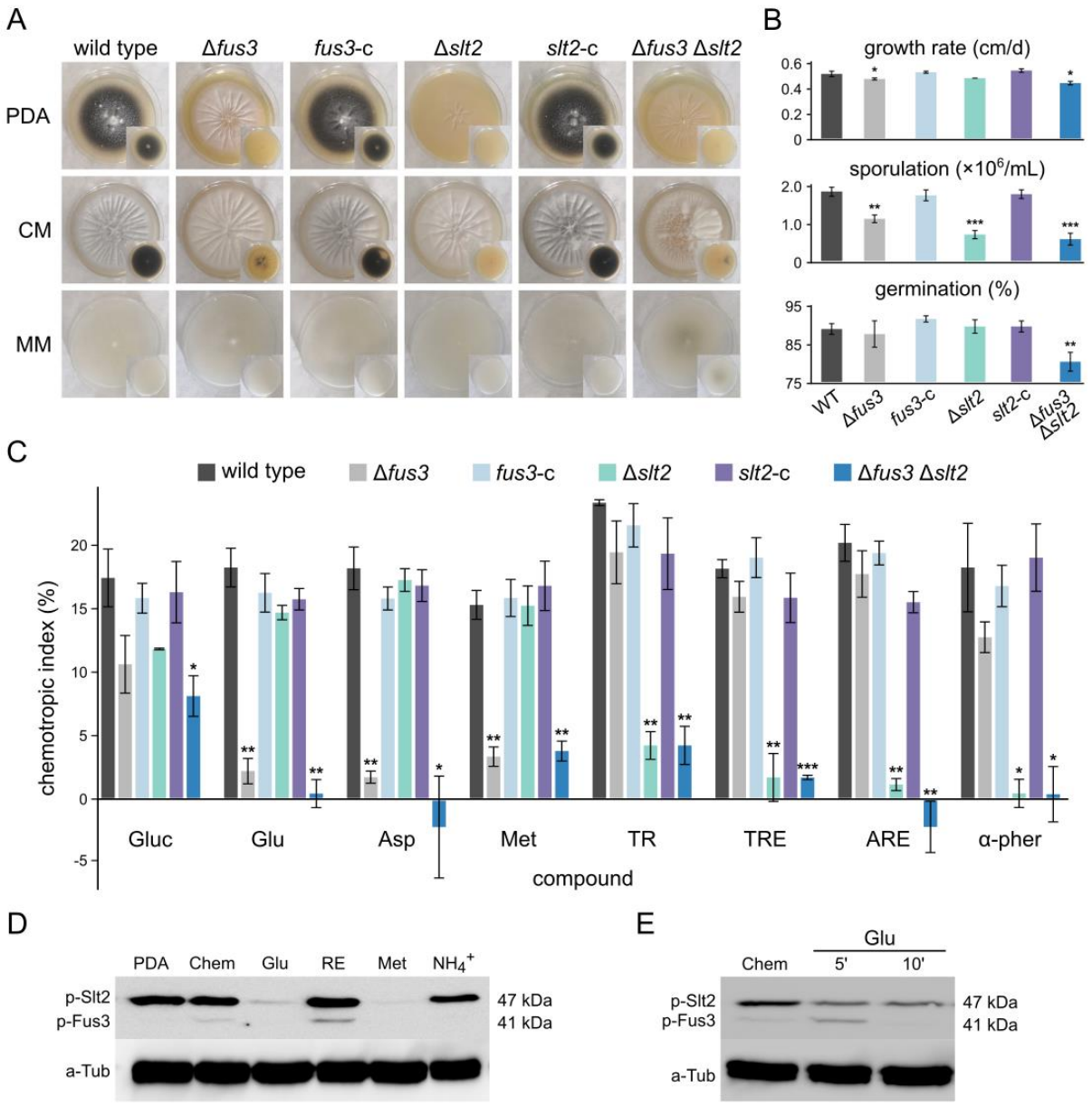

Fig. 2. The MAP kinases Fus3 and Slt2 are involved in *V. dahliae* chemotropism towards environmental nutrients and hosts/α-pheromone, respectively. **A.** Morphological features of *V. dahliae* 123V deletion mutants of *fus3* and *slt2* 35 days after inoculation on the indicated agar media. *Fus3*-c and *slt2*-c are the corresponding complemented strains. **B.** Growth rate, sporulation, and conidial germination frequency of the tested strains. **C.** Chemotropic responses of the studied mutants towards various environmental stimuli (abbreviations as in Fig. 1). In **B-C**, bars represent the SD of replicates, and statistical significance of differences from the wild type was calculated with Student's *t*-test (*$p<0.05$, **$p<0.01$, ***$p<0.001$). **D.** Western blot analysis of the phosphorylation levels of Slt2 after 15 minutes exposure to the indicated stimuli (abbreviations as in Fig. 1; PDA: potato dextrose broth; Chem: chemotropic assay medium - control). **E.** Western blot analysis of the phosphorylation levels of Slt2 at the indicated times after addition of glutamate to the culture medium.

3.3. Fus3, but not Slt2, is required for pathogenicity of V. dahliae

Our finding that Slt2 is required for chemotropism of *V. dahliae* towards the host plant led us to test the hypothesis that this MAPK might be important for pathogenicity, as previously

shown for Fus3 in a different *V. dahliae* isolate (Rauyaree et al., 2005). We therefore tested the ability of the deletion mutants to cause disease to eggplant, a particularly susceptible host of *V. dahliae* that allows convenient and reproducible scoring of disease symptoms. The results confirmed that deletion of *fus3* severely compromises pathogenicity, since plants treated with the single Δ*fus3* and the double Δ*fus3* Δ*slt2* deletion mutant showed only very mild symptoms (Fig. 3A-D). In contrast, virulence of Δ*slt2* was indistinguishable from that of the wild-type strain (Fig. 3A-D). At the end of the experiment (31 days after inoculation), measurement of the plant fresh weight and fungal re-isolation from xylem chips yielded consistent results, with Δ*fus3* and Δ*fus3* Δ*slt2* failing to reduce plant weight and rarely being recovered from the xylem of inoculated plants, whereas the results of the Δ*slt2* mutant were very similar to the wild-type levels (Fig. 3D).

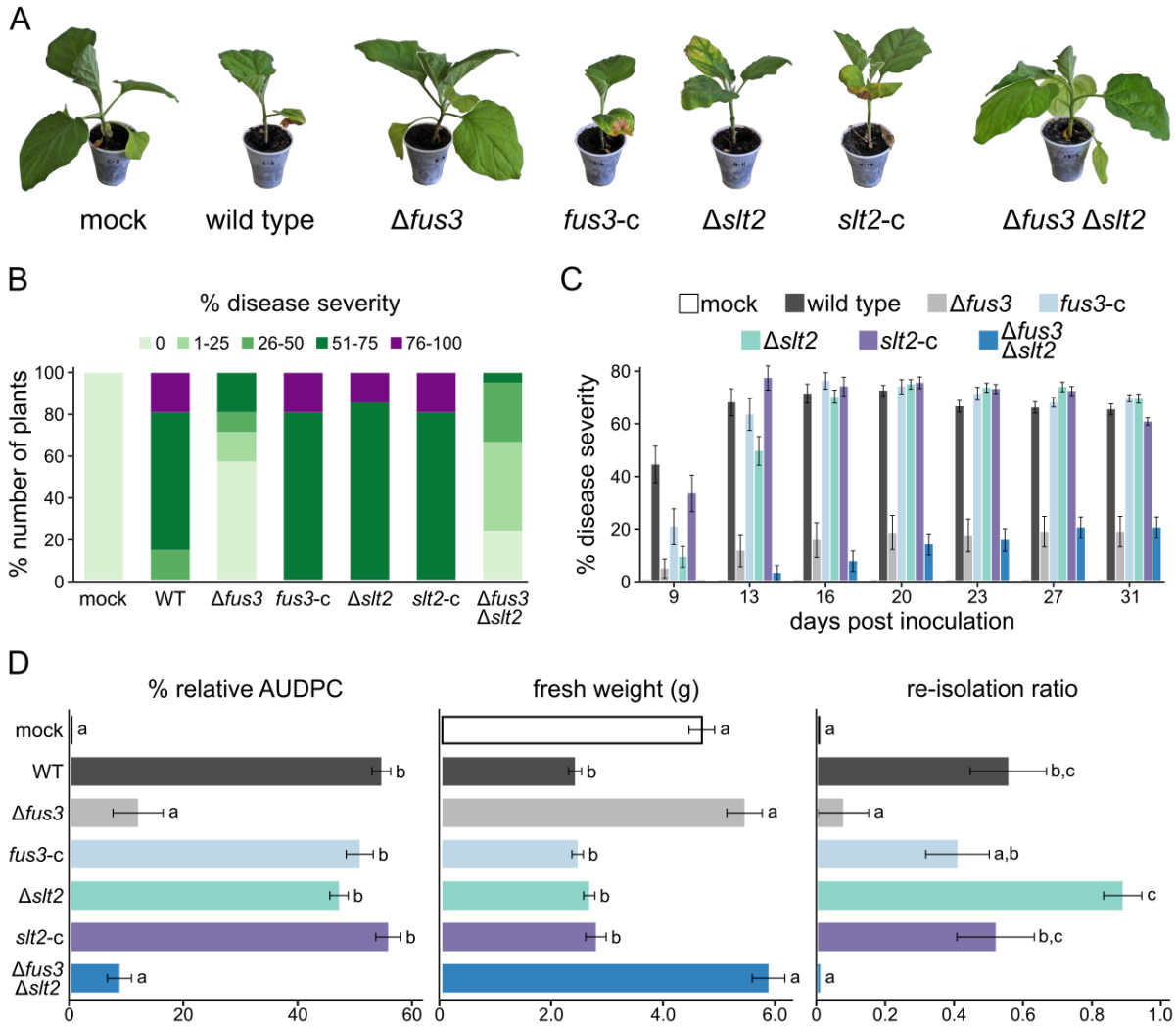

Fig. 3. Fus3, but not Slt2, is required for pathogenicity of *V. dahliae* on eggplant. **A.** Representative examples of plants inoculated with the wild-type (123V), as well as the indicated deletion mutants and complemented (*fus3*-c and *slt2*-c) strains were imaged 31 days post-inoculation (d.p.i.). **B.** Average disease severity at 31 d.p.i. (21 eggplant seedlings/strain). Non-infected plants (mock) served as controls. Percentages in different colours represent different levels of disease severity**. C.** Time-course analysis of disease severity. **D.** Mean relative area under disease progress curve (AUDPC) score for

each strain (left), average plant fresh weight (center), and fungal re-isolation ratio (right) at the end of the infection experiment (31 d.p.i.). In **C-D**, error bars represent the SE of replicates, and statistical significance of differences between strains was calculated by one-way ANOVA followed by Tukey's post hoc tests. Bars marked with the same letter do not differ significantly ($p \leq 0.05$).

3.4. Ste2 is required for chemotropism towards α-pheromone and the host plants

Binding of mating peptide pheromone to its cognate receptor (i.e., Ste2 and Ste3 in yeast) is essential for sensing mating partners and constitutes the first step in the mating pathway. Previously, the Ste2 homolog of the asexual fungal pathogen *F. oxysporum* was shown to be required for chemotropism towards α peptide pheromone and tomato root exudates (Turrà et al., 2015). We therefore tested whether Ste2 may also be involved in chemotropic sensing of *V. dahliae*.

Unlike Δ*fus3*, the Δ*ste2* mutant exhibited no visible defects in colony morphology, physiology, stress response, or pathogenicity, while the Δ*fus3* Δ*ste2* double deletion mutant displayed a similar phenotype as Δ*fus3* (Fig. 4A-C, Supplementary Fig. 2). Chemotropism assays with these mutants demonstrated that Ste2 is not required for chemosensing of different nutrients (Fig. 4D), a process that is dependent on Fus3. However, Ste2 was required for chemotropism towards tomato root exudates or *F. oxysporum* α-pheromone (Fig. 4D), similar to Slt2. The Δ*fus3* Δ*ste2* double deletion mutant showed a severely reduced chemoresponse to all tested compounds (Fig. 4D), similar to the Δ*fus3* Δ*slt2* strain. Western blot analysis revealed differences in Slt2 phosphorylation dynamics between the wild-type and the Δ*ste2* mutant upon exposure to chemotropic stimuli (Fig. 4E). Collectively, these results suggest a possible link between Ste2 and the Slt2 MAPK cascade in fungal chemosensing and chemotropism.

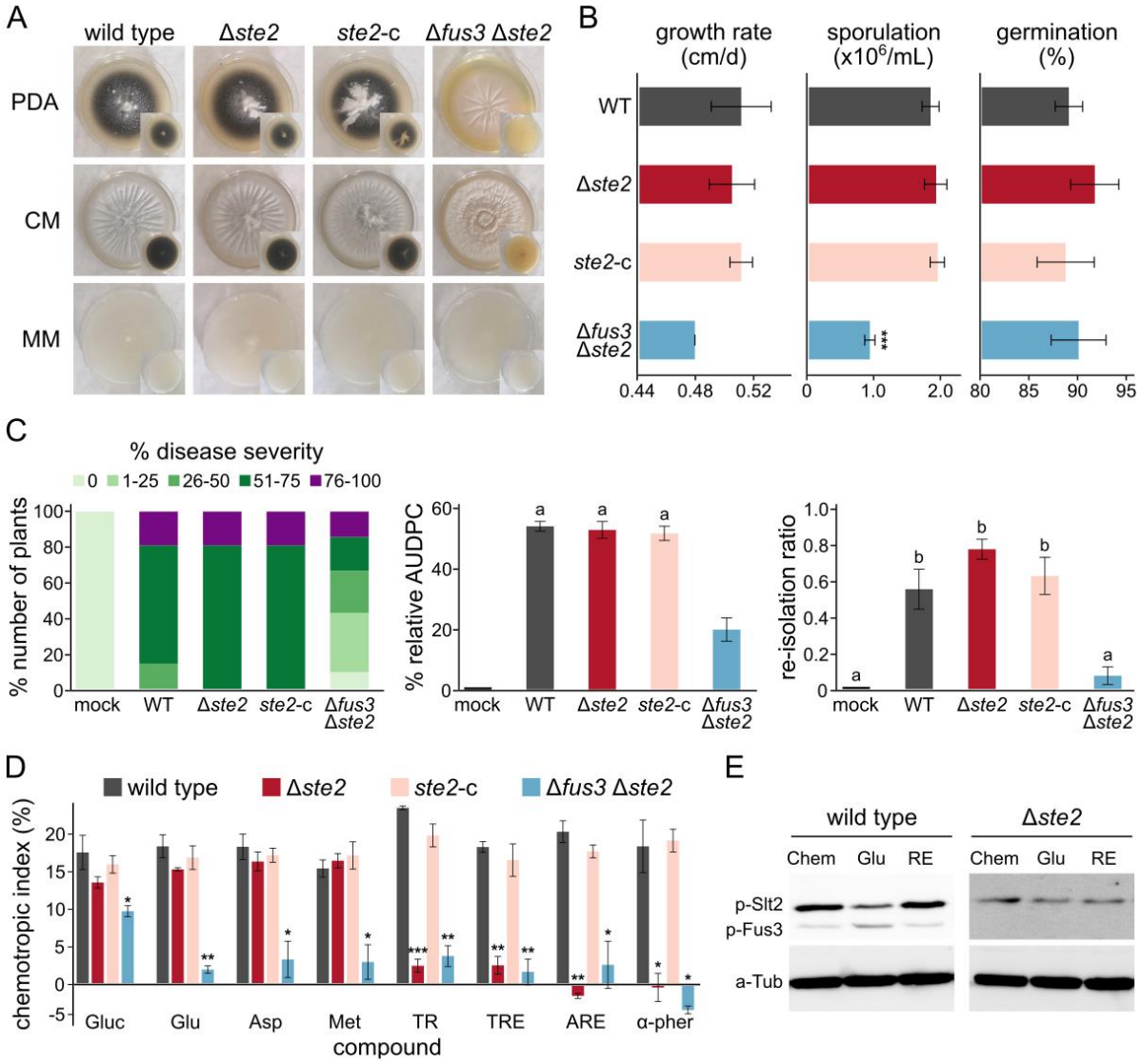

Fig. 4. Ste2 is involved in chemotropism towards hosts and α-pheromone. **A.** Morphological characteristics of *V. dahliae* 123V deletion mutants Δ*ste2* and Δ*fus3* Δ*ste2* (*ste2*-c: complemented strain) 35 days after inoculation on the indicated agar media. **B.** Growth rate, sporulation, and conidial germination frequency of the same strains. **C.** Average disease severity (left), mean relative area under disease progress curve (AUDPC) score (middle), and fungal re-isolation ratio (right) for the same *V. dahliae* strains 31 days after inoculation (21 eggplant seedlings/strain). Error bars: SE. Statistical significance of differences between strains was calculated by one-way ANOVA followed by Tukey's post hoc tests. Bars marked with the same letter did not differ significantly ($p \leq 0.05$). **D.** Chemotropic responses of the studied mutants towards various environmental stimuli (abbreviations as in Fig. 1). In **B** and **D**, bars indicate the SD of replicates, and statistical significance of differences from the wild type was calculated with Student's *t*-test (* $p \leq 0.05$, ** $p \leq 0.01$, *** $p \leq 0.001$). **E.** Western blot analysis of the phosphorylation levels of Slt2 after addition of 100 mM glutamate (Glu; 5 min) or tomato root exudate (RE; 10 min); Chem: chemotropic assay medium – control.

3.5. The TOR signaling regulators Gtr1 and Tsc2 mediate chemotropism towards nutrients and plant signals

The TOR kinase is a central molecular hub in eukaryotes where various environmental signals converge (González and Hall, 2017). Since deletion of *tor* is lethal in *V. dahliae* (Fang

et al., 2017), we performed mutational analysis of two conserved regulators of the TOR pathway, the positively acting RAG GTPase Gtr1/2 and the GTPase activating protein (GAP) Tsc1/2, which acts as a repressor of the TOR pathway (Gao et al., 2002; Valbuena et al., 2012). By using BLAST searches with the amino acid sequences of *S. cerevisiae* Gtr1 and *Sc. pombe* Tsc2 in the genome database of the *V. dahliae* reference strain Ls.17, we identified the single homologs of *gtr1* (VDAG_09326, 375 aa; 80% query coverage, 46% identity, 63% similarity) and *tsc2* (VDAG_09981, 1617 aa; 44% query coverage, 39% identity, 58% similarity). We generated Δ*gtr1* and Δ*tsc2* knockout mutants (Supplementary Fig. 1), both of which displayed reduced production of microsclerotia and limited formation of aerial mycelium (Fig. 5A), as well as lower growth rates and reduced sporulation on CM in comparison to the wild-type strain (Fig. 5B). Moreover, the Δ*tsc2* mutant exhibited defects in conidial germination (Fig. 5B). Both deletion strains showed increased sensitivity to hyperosmotic stress and to the antifungal amphotericin B, Δ*gtr1* had impaired growth in the presence of fluconazole, while Δ*tsc2* was significantly inhibited by farnesol and paraquat (Supplementary Fig. 2).

To confirm the role of these genes in TOR signaling of *V. dahliae*, we tested sensitivity of Δ*gtr1* and Δ*tsc2* to factors that induce autophagy and compared their phenotypes to that of the Δ*atg1* mutant which is impaired in autophagy (Vangalis et al., 2021b). The ability of conidia to germinate in the absence of nitrogen sources was significantly reduced in all the deletion mutants compared to the wild-type strain (Fig. 5C), consistent with a defective autophagy in the knockout mutants. Addition of different nitrogen sources fully rescued germination in both the wild-type strain and Δ*atg1,* but only partially in Δ*gtr1* and Δ*tsc2* (Fig. 5C). Treatment of conidia with rapamycin, a known inhibitor of TORC1, caused a significant and concentration-dependent reduction in germination of the Δ*gtr1*, Δ*tsc2*, and Δ*atg1* mutants but not in the wild-type and the complemented strains (Fig. 5D). These findings indicate that *V. dahliae* Gtr1 and Tsc2 are involved in regulation of TOR activity and induction of autophagy, depending on the levels of nutrient availability, consistent with their roles in other organisms (Wolfson and Sabatini, 2017).

We next asked whether Gtr1 and Tsc2 participate in the chemotropic response to nutrients and host signals. The Δ*gtr1* mutant showed a significantly reduced ability to re-direct hyphal growth towards all tested stimuli including nutrients, α-pheromone and tomato root exudate, while the Δ*tsc2* mutant showed a reduced chemotropic response to root exudate and methionine (Fig. 5E). Western blot analysis detected differential phosphorylation patterns of Slt2 upon addition of chemoattractant compounds in the Δ*gtr1* and Δ*tsc2* mutants as compared to the wild-type strain (Supplementary Fig. 3), indicating a possible crosstalk between TOR and MAPK signaling in this process.

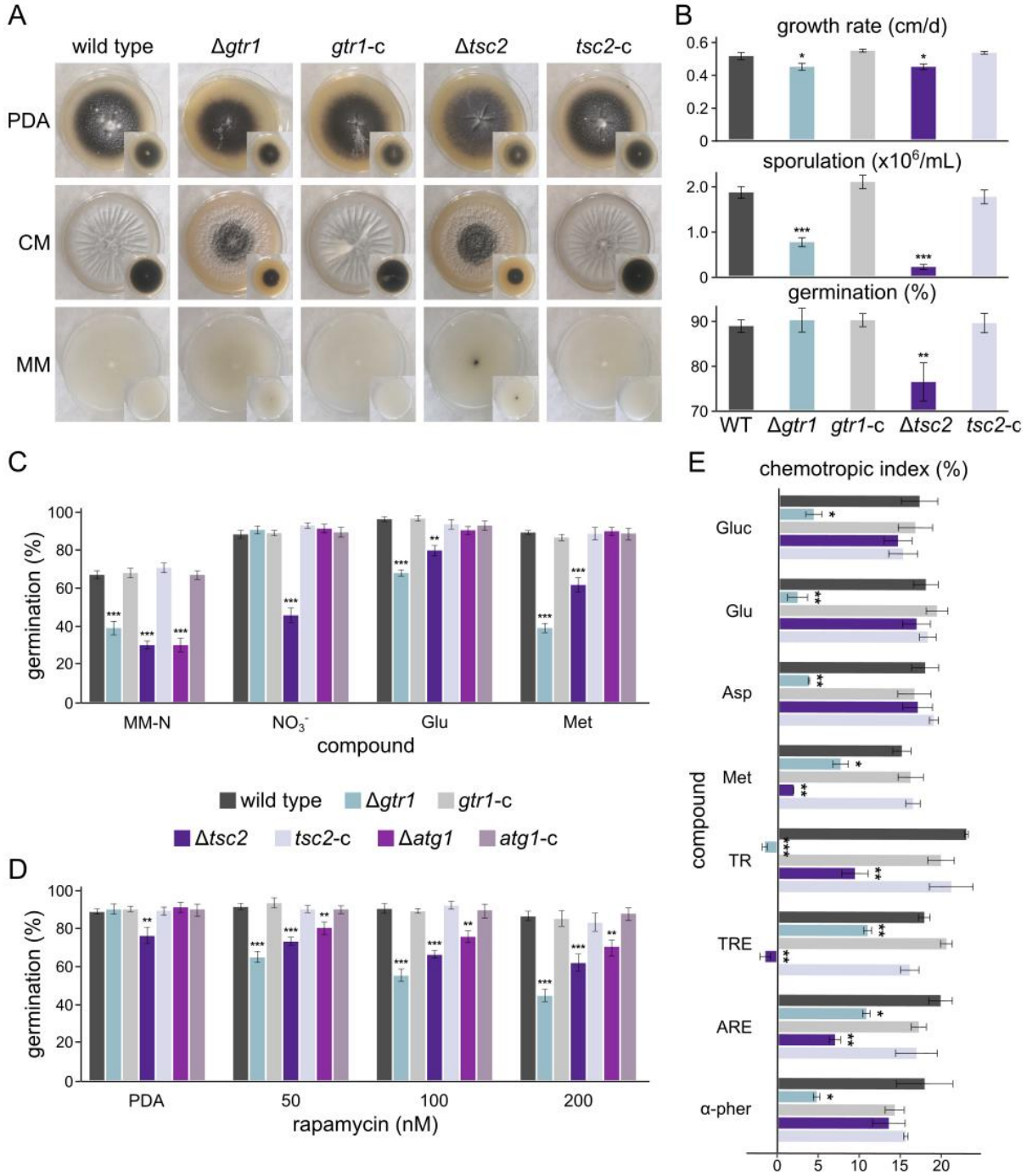

Fig. 5. Chemotropism is mediated by regulators of the TOR signaling pathway. **A.** Morphology of the *V. dahliae* wild-type (123V), Δ*gtr1*, Δ*tsc2*, and their complemented (*gtr1*-c and *tsc2*-c) strains after 35 days of growth on the indicated agar media. **B.** Growth rate, sporulation, and conidial germination frequency of the same strains. **C.** Conidial germination frequency of the indicated strains after 20 h of nitrogen starvation (MM-N) or incubation in MM supplemented with sodium nitrate (NO_3^-), glutamate (Glu), or methionine (Met). **D.** Conidial germination frequency of the indicated strains after 20 h of incubation in PDB supplemented with rapamycin. **E.** Chemotropic responses of the indicated strains 14 h after initial exposure to the indicated stimuli (for abbreviations see Fig. 1). In **B-E,** bars indicate the SD of the replicates. Statistical significance of the differences from the wild-type strain was tested with Student's *t*-test (* $p \leq 0.05$, ** $p \leq 0.01$, *** $p \leq 0.001$).

3.6. TOR signaling and autophagy control pathogenicity in V. dahliae

Pathogenicity bioassays in eggplant seedlings were performed to investigate the possible involvement of Gtr1 and Tsc2 in *V. dahliae* virulence. A small but significant decrease in the frequency of severe disease symptoms was observed in plants infected with the Δ*gtr1* and Δ*tsc2* mutants in comparison to the wild-type strain (Fig. 6A-B). A time-course comparison of symptom development revealed a delay in emergence of symptoms in the deletion mutants, with differences from the wild-type strain being more pronounced in the first 16 days after inoculation (Fig. 6C). Calculation of the average AUDPC scores over the 31 days of the experiment revealed a reduction in the Δ*gtr1* and Δ*tsc2* mutants by 33.3% and 34.8%, respectively, compared to the wild type (Fig. 6D). Moreover, the average fresh weight of plants infected with Δ*gtr1* and Δ*tsc2* was significantly lower than that of the plants treated with the wild-type strain (Fig. 6D). When we investigated the presence of the fungus within the plant tissues, the re-isolation ratio of Δ*tsc2* was significantly lower than that of the wild-type strain (Fig. 6D).

Taken together, our results show that Δ*gtr1* and Δ*tsc2* mutants are defective in regulation of TOR activity and autophagy, which has been previously shown to be important for virulence in plant-pathogenic fungi (Kershaw and Talbot, 2009; Liu et al., 2007). Therefore, we hypothesized that this dysregulation could be one of the reasons for the decreased virulence of Δ*gtr1* and Δ*tsc2*. To test whether this idea could hold true in *V. dahliae*, we investigated the pathogenic properties of the Δ*atg1* deletion strain. Our experiments demonstrated that autophagy is indeed essential for full virulence, as the deletion mutant exhibited strongly reduced disease severity (by 68.1%) and mean AUDPC score (reduced by 85.1%). Moreover, the re-isolation ratio of Δ*atg1* was reduced by 92.8%, indicating a severe defect of this mutant in systemic colonization of the host plant (Supplementary Fig. 4).

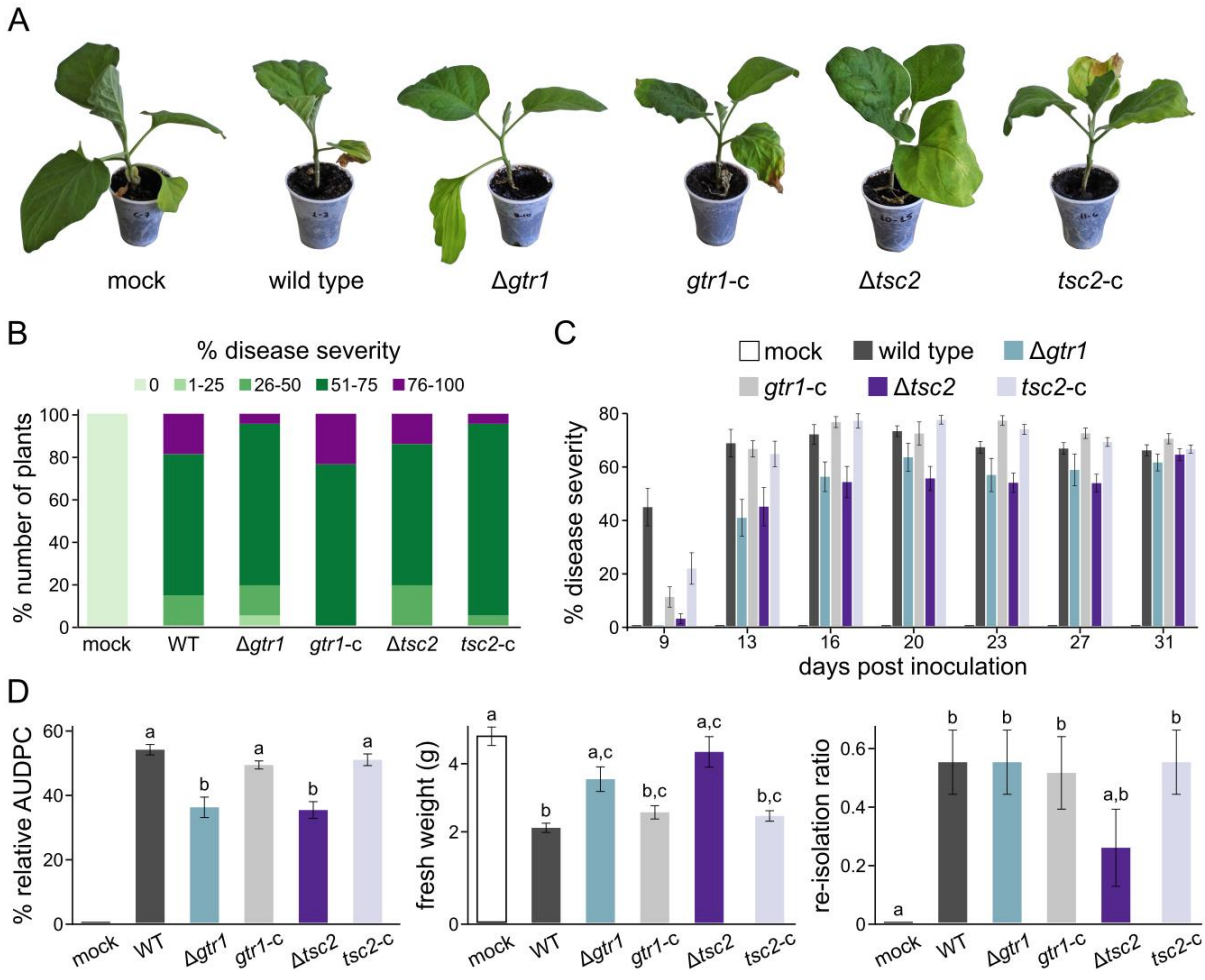

Fig. 6. The TOR signaling regulators Gtr1 and Tsc2 contribute to pathogenicity of *V. dahliae*. **A.** Representative examples of eggplant plants inoculated with the wild-type (123V), the deletion mutants, or the complemented (*gtr1*-c and *tsc2*-c) strains at 31 days post-inoculation (d.p.i.). **B.** Average disease severity at 31 d.p.i. (21 eggplant seedlings/strain). Non-inoculated plants (mock) served as controls. Percentages in different colours represent different levels of disease severity**. C.** Time-course analysis of disease severity. **D.** Mean relative AUDPC scores (left), average plant fresh weight (center), and fungal re-isolation ratios (right) at the end of the infection experiment (31 d.p.i.). In **C–D**, error bars represent the SE of replicates, and statistical significance of differences between strains was calculated by one-way ANOVA followed by Tukey's post hoc tests. Bars marked with the same letter do not differ significantly ($p \leq 0.05$).

4. Discussion

The ability of fungi to sense and grow towards environmental resources is instrumental for their growth, development, and survival. In this study we set out to elucidate the molecular mechanisms that govern chemotropic responses during hyphal growth and host interactions of the important plant pathogen *V. dahliae*. To this end, a chemotropism assay on agar plates (Turrà et al., 2015) was optimized for *V. dahliae* enabling reproducible quantification of chemotropic hyphal growth towards a variety of environmental signals.

Our experiments revealed that *V. dahliae* germlings can readily sense and re-orient growth of their hyphal tips towards different carbon and nitrogen sources, similar to what has been previously reported in *F. oxysporum* and *F. graminearum* (Sridhar et al., 2020; Turrà et al., 2015). Nitrogen availability is particularly important for plant pathogenicity (Deng et al., 2015), and the ability of the pathogen to sense and reach suitable nitrogen sources is likely to be important for successful host invasion (Thalineau et al., 2016). Here we found that *V. dahliae* exhibits robust chemotropic responses towards extracellular signals from plant roots. The disease cycle of this fungus normally starts when germination of its resting structures (i.e., microsclerotia) in the soil is triggered by the presence of plant roots nearby, followed by directed hyphal growth towards the roots and invasion. The underlying sensing and chemotropic machinery is therefore essential for pathogenesis. In *F. oxysporum*, which also invades plant roots, chemotropism towards roots is mediated by secreted root peroxidases (Turrà et al., 2015; Nordzieke et al., 2019), and this could be a conserved mechanism for root-invading fungi. Interestingly, our assay also revealed strong chemotropic responses of *V. dahliae* towards the peptide α-pheromone of *F. oxysporum*. Although both fungi are regarded as asexual, our recent investigations showed that *V. dahliae* frequently engages in vegetative hyphal fusions that lead to the formation of viable heterokaryons (Vangalis et al., 2021b). Moreover, genomic evidence for horizontal gene transfer from *F. oxysporum* to *V. dahliae* has been reported (Chen et al., 2018). We speculate that under particular selective conditions the two species might be able to undergo vegetative fusion or communicate via physical cell contact (Haj Hammadeh et al., 2022), and that their pheromone-sensing systems might mediate such interspecific interactions.

The TOR kinase is a central molecular hub that coordinates responses to the availability of various environmental resources in eukaryotes from yeast to mammals (González and Hall, 2017). In this study, functional characterization of the *V. dahliae* homologs of Gtr1 and Tsc2, two conserved components of the TOR pathway, revealed a role of TOR signaling in sensing and chemotropic growth towards various environmental stimuli. Particularly Gtr1 was important for chemotropic responses towards all the tested stimuli, indicating that the Rag GTPase Gtr1/2 complex plays a central role in the chemosensing process. The mammalian

homolog RagA/B-RagC/D, is responsible for activation of mTORC1 upon nutrient availability by translocating mTORC1 to the lysosomal surface (Wolfson and Sabatini, 2017). Our results indicate that this function could be conserved in filamentous fungi. On the other hand, Tsc1/2 complex is a TOR repressor that acts under conditions of amino acid deprivation and cellular stress (Gao et al., 2002). Deletion of *V. dahliae tsc2* rendered the fungus unable to re-direct growth towards host-derived signals and the amino acid methionine, but not towards other nutrient sources. Because intracellular amino acid sensors are not conserved across eukaryotes (Wolfson and Sabatini, 2017), filamentous fungi may have evolved different mechanisms, some of which may involve the Tsc1/2 complex. For example, deletion of *tsc1* or *tsc2* in *Sc. pombe* compromises uptake of arginine and other amino acids, and deletion mutants exhibit decreased expression of amino acid permeases as well as deficiencies in the arginine biosynthesis pathway (Matsumoto et al., 2002; Slegtenhorst et al., 2004). Notably, the Tsc1/2 complex has been implicated in polarization of macrophages upon IL-4 induction (Byles et al., 2013). Together with our results, this points towards a conserved role of the Tsc1/2-TOR system in sensing of a variety of environmental signals and in mediating targeted cellular responses.

In addition to their role in chemotropism, *gtr1* and *tsc2* were required for normal morphogenesis, physiology, and stress response, indicating a conserved role of the TOR signaling pathway in fungal development (Yu et al., 2014). The conidial germination defect of the Δ*tsc2* mutant could be attributed to its inability to undergo autophagy, a process that was shown to be important for conidial germination (Kikuma et al., 2006; Vangalis et al., 2021b). Besides the contributions of Gtr1 and Tsc2 to fungal chemotropism towards root signals and other developmental processes, both components were found to be required for full virulence of *V. dahliae* on eggplants, further supporting a conserved role of TOR signaling in virulence of fungal plant pathogens (Li et al., 2019; Yu et al., 2014). In the case of Tsc2, we hypothesize that its known role in induction of autophagy (Ng et al., 2011), which is further supported by our results, may explain the compromised pathogenicity of the deletion mutant. Consistent with this idea, deletion of *V. dahliae atg1* also resulted in severely decreased virulence, in agreement with findings in other plant pathogens such as *M. oryzae* (Kershaw and Talbot, 2009; Liu et al., 2007). We thus propose that *V. dahliae* Tsc1/2 regulates multiple processes associated with plant pathogenicity, including chemotropism towards roots, fungal development within the host, and autophagy.

To gain a more complete understanding of the signaling components that control *V. dahliae* chemotropism, we used our optimized assay to investigate the role of MAPK signaling. We found that the MAPK Fus3 controls chemotropism towards nutrients, while the GPCR Ste2 and the MAPK Slt2 mediate chemotropic sensing of root signals and α-pheromone. These results are in agreement with previous findings in *F. oxysporum* (Turrà et al., 2015) and

reveal that, in contrast to the well-characterized functional association of Ste2 and Fus3 in the yeast mating pathway (Merlini et al., 2013), these asexual fungi employ different associations in processes other than mating, such as Ste2-Slt2 for host and intra-species sensing and Fus3 with unknown receptors for nutrient sensing. Further supporting this notion, Fus3 was also functionally uncoupled from Ste2 in conidial and hyphal fusion of filamentous fungi, including *V. dahliae* (Fischer and Glass, 2019; Vangalis et al., 2021a).

In the light of the involvement of both TOR and MAPK signaling in *V. dahliae* chemotropism, an interesting question is whether and how these two pathways interact with each other to control the process. Crosstalk between TOR and MAPK pathways have been reported in fission yeast, where it was proposed to mediate cellular adaptation to multiple environmental cues (Madrid et al., 2016). In *F. oxysporum,* indirect indications of a crosstalk between TOR and the Fus3 homolog, Fmk1, has been reported during regulation of virulence in response to nitrogen sources (López-Berges et al., 2010). Our preliminary results showing altered patterns of Slt2 phosphorylation in the Δ*gtr1* and Δ*tsc2* mutants also point towards a possible crosstalk between TOR and MAPK pathways in chemotropic signaling. We hypothesize that the TOR pathway might be transducing environmental signals to the MAPK cascades for downstream signal processing and cellular responses.

Deletion of *slt2* resulted in a complete absence of microsclerotia and other morphological and physiological defects, as well as increased sensitivity to cell wall stress. These results are consistent with the known role of Slt2 in preserving cell wall integrity, and are in agreement with similar phenotypes reported in other plant pathogens (Jiang et al., 2018). Despite these defects and the role of Slt2 role in sensing of plant roots, deletion of *slt2* had no significant effect on virulence in our assay conditions, and the same result was obtained for the Δ*ste2* mutant. On the contrary, deletion of any of these two components in *F. oxysporum* resulted in reduced virulence (Segorbe et al., 2017; Turrà et al., 2015). Future investigations are required to clarify whether this discrepancy may reflect genetic or regulatory differences between these two species, or whether it may be due to differences in the bioassays used to determine virulence, for example the amount of fungal inoculum. In contrast to Slt2 and Ste2, our results with the Δ*fus3* mutant fully corroborate previous results showing that this MAPK is essential for pathogenicity of *V. dahliae* (Rauyaree et al., 2005), a role that is conserved in all other fungal phytopathogens analyzed so far (Jiang et al., 2018; Turrà et al., 2014).

5. Conclusion

Our study establishes the important plant-pathogenic fungus *V. dahliae* as a suitable model for studying the mechanisms of environmental sensing and chemotropism during hyphal growth and host-pathogen interactions. The TOR signaling pathway was shown for the first time to play an important role in chemotropism, along with an involvement in fungal development and virulence. In addition, members of MAPK cascades were found to have conserved roles in chemotropism towards different types of environmental signals, as well as important functions in fungal biology and pathogenicity. Our study contributes to the understanding of the complex chemosensing mechanisms in fungi and raises new questions for future research.

Acknowledgements

We wish to thank Malena P. Pantou for the Δ*fus3* mutant, which was constructed during her previous work in the laboratory of Milton A. Typas, as well as Melani Mariscal Gómez and Rafael Palos Fernández from the University of Córdoba for their helpful instructions with the plate chemotropism assay.

Funding

We are grateful to the Federation of European Microbiological Societies (FEMS) for awarding Vasileios Vangalis with a Research and Training Grant that funded his visit to the laboratory of Antonio Di Pietro to conduct part of this research. Research in the Di Pietro lab was funded by grants from the Spanish Ministry of Science and Innovation (MICINN, grant PID2019-108045RB-I00) and Junta de Andalucía (P20_00179).

Declaration of Competing Interest

The authors declare no conflict of interest.

Authors contribution statement

Vasileios Vangalis: Conceptualization, Methodology, Investigation, Data curation, Formal analysis, Visualization, Writing – original draft, Writing – review and editing.

Emmanouil A. Markakis: Methodology, Investigation, Formal analysis, Writing – review and editing.

Michael Knop: Funding acquisition, Writing – review and editing.

Antonio Di Pietro: Methodology, Supervision, Resources, Funding acquisition, Writing – review and editing.

Milton A. Typas: Methodology, Supervision, Resources, Funding acquisition, Writing – review and editing.

Ioannis A. Papaioannou: Conceptualization, Methodology, Supervision, Writing – original draft, Writing – review and editing.

Appendix A. Supplementary Material

Supplementary material related to this article can be found, in the online version, at doi:XXX

References

Binda, M., Péli-Gulli, M.-P., Bonfils, G., Panchaud, N., Urban, J., Sturgill, T.W., Loewith, R., Virgilio, C.D., 2009. The Vam6 GEF Controls TORC1 by Activating the EGO Complex. Molecular Cell 35, 563–573. https://doi.org/10.1016/j.molcel.2009.06.033

Brand, A., Gow, N.A., 2009. Mechanisms of hypha orientation of fungi. Current Opinion in Microbiology, Host–Microbe Interactions: Fungi/Parasites/Viruses 12, 350–357. https://doi.org/10.1016/j.mib.2009.05.007

Byles, V., Covarrubias, A.J., Ben-Sahra, I., Lamming, D.W., Sabatini, D.M., Manning, B.D., Horng, T., 2013. The TSC-mTOR pathway regulates macrophage polarization. Nat Commun 4, 2834. https://doi.org/10.1038/ncomms3834

Chantranupong, L., Wolfson, R.L., Sabatini, D.M., 2015. Nutrient-Sensing Mechanisms across Evolution. Cell 161, 67–83. https://doi.org/10.1016/j.cell.2015.02.041

Chen, J.-Y., Liu, C., Gui, Y.-J., Si, K.-W., Zhang, D.-D., Wang, J., Short, D.P.G., Huang, J.-Q., Li, N.-Y., Liang, Y., Zhang, W.-Q., Yang, L., Ma, X.-F., Li, T.-G., Zhou, L., Wang, B.-L., Bao, Y.-M., Subbarao, K.V., Zhang, G.-Y., Dai, X.-F., 2018. Comparative genomics reveals cotton-specific virulence factors in flexible genomic regions in Verticillium dahliae and evidence of horizontal gene transfer from Fusarium. New Phytol 217, 756–770. https://doi.org/10.1111/nph.14861

Deng, Y., Yang, F., Naqvi, N.I., 2015. The role of nutrients in fungal development and pathogenesis, in: Fungal Biomolecules. John Wiley & Sons, Ltd, pp. 201–211. https://doi.org/10.1002/9781118958308.ch15

Dobrenel, T., Caldana, C., Hanson, J., Robaglia, C., Vincentz, M., Veit, B., Meyer, C., 2016. TOR Signaling and Nutrient Sensing. Annual Review of Plant Biology 67, 261–285. https://doi.org/10.1146/annurev-arplant-043014-114648

Fang, Y., Xiong, D., Tian, L., Tang, C., Wang, Y., Tian, C., 2017. Functional characterization of two bZIP transcription factors in Verticillium dahliae. Gene 626, 386–394. https://doi.org/10.1016/j.gene.2017.05.061

Fischer, M.S., Glass, N.L., 2019. Communicate and Fuse: How Filamentous Fungi Establish and Maintain an Interconnected Mycelial Network. Front Microbiol 10, 619. https://doi.org/10.3389/fmicb.2019.00619

685 Fitzgibbon, G.J., Morozov, I.Y., Jones, M.G., Caddick, M.X., 2005. Genetic Analysis of the TOR
686 Pathway in Aspergillus nidulans. Eukaryot Cell 4, 1595–1598.
687 https://doi.org/10.1128/EC.4.9.1595-1598.2005
688 Fleissner, A., Leeder, A.C., Roca, M.G., Read, N.D., Glass, N.L., 2009. Oscillatory recruitment of
689 signaling proteins to cell tips promotes coordinated behavior during cell fusion. PNAS 106,
690 19387–19392. https://doi.org/10.1073/pnas.0907039106
691 Gao, X., Zhang, Y., Arrazola, P., Hino, O., Kobayashi, T., Yeung, R.S., Ru, B., Pan, D., 2002. Tsc tumour
692 suppressor proteins antagonize amino-acid-TOR signalling. Nat Cell Biol 4, 699–704.
693 https://doi.org/10.1038/ncb847
694 González, A., Hall, M.N., 2017. Nutrient sensing and TOR signaling in yeast and mammals. EMBO J
695 36, 397–408. https://doi.org/10.15252/embj.201696010
696 Haj Hammadeh, H., Serrano, A., Wernet, V., Stomberg, N., Hellmeier, D., Weichert, M., Brandt, U.,
697 Sieg, B., Kanofsky, K., Hehl, R., Fischer, R., Fleißner, A., 2022. A dialogue-like cell
698 communication mechanism is conserved in filamentous ascomycete fungi and mediates
699 interspecies interactions. Proceedings of the National Academy of Sciences 119,
700 e2112518119. https://doi.org/10.1073/pnas.2112518119
701 Jiang, C., Zhang, X., Liu, H., Xu, J.-R., 2018. Mitogen-activated protein kinase signaling in plant
702 pathogenic fungi. PLOS Pathogens 14, e1006875.
703 https://doi.org/10.1371/journal.ppat.1006875
704 Kershaw, M.J., Talbot, N.J., 2009. Genome-wide functional analysis reveals that infection-associated
705 fungal autophagy is necessary for rice blast disease. PNAS 106, 15967–15972.
706 https://doi.org/10.1073/pnas.0901477106
707 Kikuma, T., Ohneda, M., Arioka, M., Kitamoto, K., 2006. Functional Analysis of the ATG8 Homologue
708 Aoatg8 and Role of Autophagy in Differentiation and Germination in Aspergillus oryzae.
709 Eukaryotic Cell 5, 1328–1336. https://doi.org/10.1128/EC.00024-06
710 Kira, S., Kumano, Y., Ukai, H., Takeda, E., Matsuura, A., Noda, T., 2016. Dynamic relocation of the
711 TORC1-Gtr1/2-Ego1/2/3 complex is regulated by Gtr1 and Gtr2. Mol Biol Cell 27, 382–396.
712 https://doi.org/10.1091/mbc.E15-07-0470
713 Kira, S., Tabata, K., Shirahama-Noda, K., Nozoe, A., Yoshimori, T., Noda, T., 2014. Reciprocal
714 conversion of Gtr1 and Gtr2 nucleotide-binding states by Npr2-Npr3 inactivates TORC1 and
715 induces autophagy. Autophagy 10, 1565–1578. https://doi.org/10.4161/auto.29397
716 Klosterman, S.J., Atallah, Z.K., Vallad, G.E., Subbarao, K.V., 2009. Diversity, Pathogenicity, and
717 Management of Verticillium Species. Annual Review of Phytopathology 47, 39–62.
718 https://doi.org/10.1146/annurev-phyto-080508-081748
719 Leeder, A.C., Palma-Guerrero, J., Glass, N.L., 2011. The social network: deciphering fungal language.
720 Nature Reviews Microbiology 9, 440. https://doi.org/10.1038/nrmicro2580
721 Li, L., Zhu, T., Song, Y., Luo, X., Feng, L., Zhuo, F., Li, F., Ren, M., 2019. Functional Characterization of
722 Target of Rapamycin Signaling in Verticillium dahliae. Front Microbiol 10, 501.
723 https://doi.org/10.3389/fmicb.2019.00501
724 Liu, X.-H., Lu, J.-P., Zhang, L., Dong, B., Min, H., Lin, F.-C., 2007. Involvement of a Magnaporthe grisea
725 serine/threonine kinase gene, MgATG1, in appressorium turgor and pathogenesis. Eukaryot
726 Cell 6, 997–1005. https://doi.org/10.1128/EC.00011-07
727 Lombardi, N., Vitale, S., Turrà, D., Reverberi, M., Fanelli, C., Vinale, F., Marra, R., Ruocco, M., Pascale,
728 A., d'Errico, G., Woo, S.L., Lorito, M., 2018. Root Exudates of Stressed Plants Stimulate and
729 Attract Trichoderma Soil Fungi. MPMI 31, 982–994. https://doi.org/10.1094/MPMI-12-17-
730 0310-R
731 López-Berges, M.S., Rispail, N., Prados-Rosales, R.C., Di Pietro, A., 2010. A nitrogen response
732 pathway regulates virulence functions in Fusarium oxysporum via the protein kinase TOR
733 and the bZIP protein MeaB. Plant Cell 22, 2459–2475.
734 https://doi.org/10.1105/tpc.110.075937

735 Lu, S., Lyngholm, L., Yang, G., Bronson, C., Yoder, O.C., Turgeon, B.G., 1994. Tagged mutations at the
736 Tox1 locus of Cochliobolus heterostrophus by restriction enzyme-mediated integration.
737 Proc. Natl. Acad. Sci. U.S.A. 91, 12649–12653. https://doi.org/10.1073/pnas.91.26.12649
738 Madrid, M., Vázquez-Marín, B., Franco, A., Soto, T., Vicente-Soler, J., Gacto, M., Cansado, J., 2016.
739 Multiple crosstalk between TOR and the cell integrity MAPK signaling pathway in fission
740 yeast. Sci Rep 6, 37515. https://doi.org/10.1038/srep37515
741 Markakis, E.A., Ligoxigakis, E.K., Avramidou, E.V., Tzanidakis, N., 2014. Survival, Persistence, and
742 Infection Efficiency of Verticillium dahliae Passed Through the Digestive System of Sheep.
743 Plant Dis. 98, 1235–1240. https://doi.org/10.1094/PDIS-12-13-1201-RE
744 Matsumoto, S., Bandyopadhyay, A., Kwiatkowski, D.J., Maitra, U., Matsumoto, T., 2002. Role of the
745 Tsc1-Tsc2 complex in signaling and transport across the cell membrane in the fission yeast
746 Schizosaccharomyces pombe. Genetics 161, 1053–1063.
747 https://doi.org/10.1093/genetics/161.3.1053
748 Méchin, V., Damerval, C., Zivy, M., 2007. Total protein extraction with TCA-acetone. Methods Mol
749 Biol 355, 1–8. https://doi.org/10.1385/1-59745-227-0:1
750 Merlini, L., Dudin, O., Martin, S.G., 2013. Mate and fuse: how yeast cells do it. Open Biol 3, 130008.
751 https://doi.org/10.1098/rsob.130008
752 Moreno-Ruiz, D., Lichius, A., Turrà, D., Di Pietro, A., Zeilinger, S., 2020. Chemotropism Assays for
753 Plant Symbiosis and Mycoparasitism Related Compound Screening in Trichoderma
754 atroviride. Front Microbiol 11, 601251. https://doi.org/10.3389/fmicb.2020.601251
755 Ng, S., Wu, Y.-T., Chen, B., Zhou, J., Shen, H.-M., 2011. Impaired autophagy due to constitutive mTOR
756 activation sensitizes TSC2-null cells to cell death under stress. Autophagy 7, 1173–1186.
757 https://doi.org/10.4161/auto.7.10.16681
758 Nguyen, Q.B., Kadotani, N., Kasahara, S., Tosa, Y., Mayama, S., Nakayashiki, H., 2008. Systematic
759 functional analysis of calcium-signalling proteins in the genome of the rice-blast fungus,
760 Magnaporthe oryzae, using a high-throughput RNA-silencing system. Molecular
761 Microbiology 68, 1348–1365. https://doi.org/10.1111/j.1365-2958.2008.06242.x
762 Nordzieke, D.E., Fernandes, T.R., Ghalid, M.E., Turrà, D., Pietro, A.D., 2019. NADPH oxidase regulates
763 chemotropic growth of the fungal pathogen Fusarium oxysporum towards the host plant.
764 New Phytologist 224, 1600–1612. https://doi.org/10.1111/nph.16085
765 Papaioannou, I.A., Ligoxigakis, E.K., Vakalounakis, D.J., Markakis, E.A., Typas, M.A., 2013.
766 Phytopathogenic, morphological, genetic and molecular characterization of a Verticillium
767 dahliae population from Crete, Greece. Eur J Plant Pathol 136, 577–596.
768 https://doi.org/10.1007/s10658-013-0189-4
769 Paz, Z., García-Pedrajas, M.D., Andrews, D.L., Klosterman, S.J., Baeza-Montañez, L., Gold, S.E., 2011.
770 One Step Construction of Agrobacterium-Recombination-ready-plasmids (OSCAR), an
771 efficient and robust tool for ATMT based gene deletion construction in fungi. Fungal
772 Genetics and Biology, Special Section: Fungal Mating 48, 677–684.
773 https://doi.org/10.1016/j.fgb.2011.02.003
774 Pegg, G.F, Brady, B.L., 2002. Verticillium wilts. [WWW Document]. URL
775 https://www.cabi.org/isc/abstract/20023073035 (accessed 6.5.21).
776 Rauyaree, P., Ospina-Giraldo, M.D., Kang, S., Bhat, R.G., Subbarao, K.V., Grant, S.J., Dobinson, K.F.,
777 2005. Mutations in VMK1, a mitogen-activated protein kinase gene, affect microsclerotia
778 formation and pathogenicity in Verticillium dahliae. Curr Genet 48, 109–116.
779 https://doi.org/10.1007/s00294-005-0586-0
780 Riquelme, M., 2013. Tip Growth in Filamentous Fungi: A Road Trip to the Apex. Annual Review of
781 Microbiology 67, 587–609. https://doi.org/10.1146/annurev-micro-092412-155652
782 Saxton, R.A., Sabatini, D.M., 2017. mTOR Signaling in Growth, Metabolism, and Disease. Cell 168,
783 960–976. https://doi.org/10.1016/j.cell.2017.02.004
784 Segorbe, D., Di Pietro, A., Pérez-Nadales, E., Turrà, D., 2017. Three Fusarium oxysporum mitogen-
785 activated protein kinases (MAPKs) have distinct and complementary roles in stress

786 adaptation and cross-kingdom pathogenicity. Mol Plant Pathol 18, 912–924.
787 https://doi.org/10.1111/mpp.12446
788 Slegtenhorst, M. van, Carr, E., Stoyanova, R., Kruger, W.D., Henske, E.P., 2004. Tsc1+ and tsc2+
789 Regulate Arginine Uptake and Metabolism in Schizosaccharomyces pombe*. Journal of
790 Biological Chemistry 279, 12706–12713. https://doi.org/10.1074/jbc.M313874200
791 Sridhar, P.S., Trofimova, D., Subramaniam, R., González-Peña Fundora, D., Foroud, N.A., Allingham,
792 J.S., Loewen, M.C., 2020. Ste2 receptor-mediated chemotropism of Fusarium graminearum
793 contributes to its pathogenicity against wheat. Sci Rep 10, 10770.
794 https://doi.org/10.1038/s41598-020-67597-z
795 Thalineau, E., Truong, H.-N., Berger, A., Fournier, C., Boscari, A., Wendehenne, D., Jeandroz, S., 2016.
796 Cross-Regulation between N Metabolism and Nitric Oxide (NO) Signaling during Plant
797 Immunity. Frontiers in Plant Science 7.
798 Turrà, D., El Ghalid, M., Rossi, F., Di Pietro, A., 2015. Fungal pathogen uses sex pheromone receptor
799 for chemotropic sensing of host plant signals. Nature 527, 521–524.
800 https://doi.org/10.1038/nature15516
801 Turrà, D., Nordzieke, D., Vitale, S., El Ghalid, M., Di Pietro, A., 2016. Hyphal chemotropism in fungal
802 pathogenicity. Seminars in Cell & Developmental Biology, Transcriptional Enhancers 57, 69–
803 75. https://doi.org/10.1016/j.semcdb.2016.04.020
804 Turrà, D., Segorbe, D., Di Pietro, A., 2014. Protein kinases in plant-pathogenic fungi: conserved
805 regulators of infection. Annu Rev Phytopathol 52, 267–288.
806 https://doi.org/10.1146/annurev-phyto-102313-050143
807 Valbuena, N., Guan, K.-L., Moreno, S., 2012. The Vam6 and Gtr1–Gtr2 pathway activates TORC1 in
808 response to amino acids in fission yeast. Journal of Cell Science 125, 1920–1928.
809 https://doi.org/10.1242/jcs.094219
810 Van Dijck, P., Brown, N.A., Goldman, G.H., Rutherford, J., Xue, C., Van Zeebroeck, G., 2017. Nutrient
811 Sensing at the Plasma Membrane of Fungal Cells. Microbiol Spectr 5.
812 https://doi.org/10.1128/microbiolspec.FUNK-0031-2016
813 Vangalis, V., Knop, M., Typas, M.A., Papaioannou, I.A., 2021a. Establishment of conidial fusion in the
814 asexual fungus Verticillium dahliae as a useful system for the study of non-sexual genetic
815 interactions. Curr Genet 67, 471–485. https://doi.org/10.1007/s00294-021-01157-4
816 Vangalis, V., Likhotkin, I., Knop, M., Typas, M.A., Papaioannou, I.A., 2021b. Starvation-induced cell
817 fusion and heterokaryosis frequently escape imperfect allorecognition systems in an asexual
818 fungal pathogen. BMC Biology 19, 169. https://doi.org/10.1186/s12915-021-01101-5
819 Vangalis, V., Papaioannou, I.A., Markakis, E.A., Knop, M., Typas, M.A., 2021c. The NADPH Oxidase A
820 of Verticillium dahliae Is Essential for Pathogenicity, Normal Development, and Stress
821 Tolerance, and It Interacts with Yap1 to Regulate Redox Homeostasis. J Fungi (Basel) 7, 740.
822 https://doi.org/10.3390/jof7090740
823 Vangalis, V., Papaioannou, I.A., Markakis, E.A., Knop, M., Typas, M.A., 2020. Hex1, the Major
824 Component of Woronin Bodies, Is Required for Normal Development, Pathogenicity, and
825 Stress Response in the Plant Pathogenic Fungus Verticillium dahliae. Journal of Fungi 6, 344.
826 https://doi.org/10.3390/jof6040344
827 Vitale, S., Di Pietro, A., Turrà, D., 2019. Autocrine pheromone signalling regulates community
828 behaviour in the fungal pathogen Fusarium oxysporum. Nat Microbiol 4, 1443–1449.
829 https://doi.org/10.1038/s41564-019-0456-z
830 Weisman, R., 2016. Target of Rapamycin (TOR) Regulates Growth in Response to Nutritional Signals.
831 Microbiol Spectr 4. https://doi.org/10.1128/microbiolspec.FUNK-0006-2016
832 Wolfson, R.L., Sabatini, D.M., 2017. The Dawn of the Age of Amino Acid Sensors for the mTORC1
833 Pathway. Cell Metab 26, 301–309. https://doi.org/10.1016/j.cmet.2017.07.001
834 Workman, J.J., Chen, H., Laribee, R.N., 2014. Environmental signaling through the mechanistic target
835 of rapamycin complex 1: mTORC1 goes nuclear. Cell Cycle 13, 714–725.
836 https://doi.org/10.4161/cc.28112

Yu, F., Gu, Q., Yun, Y., Yin, Y., Xu, J.-R., Shim, W.-B., Ma, Z., 2014. The TOR signaling pathway regulates vegetative development and virulence in Fusarium graminearum. New Phytol 203, 219–232. https://doi.org/10.1111/nph.12776

Zhao, X., Mehrabi, R., Xu, J.-R., 2007. Mitogen-Activated Protein Kinase Pathways and Fungal Pathogenesis. Eukaryot Cell 6, 1701–1714. https://doi.org/10.1128/EC.00216-07

Supplementary Information

Components of TOR and MAP kinase signaling control chemotropism and pathogenicity in a fungal pathogen

V. Vangalis, E. A. Markakis, M. Knop, A. Di Pietro, M. A. Typas, I. A. Papaioannou

Supplementary Table 1. *Verticillium dahliae* strains used in this study.

strain	background	genotype	constructed using plasmid(s)
123V	-	wild type	–
123V-Δfus3	123V	*fus3*::*hph*	pUCfus3
123V-fus3-c	123V-Δfus3	*fus3*::*hph*, *fus3*, *neo*^{R}	pUCfus3, fus3, pSD1
123V-Δslt2	123V	Δ*slt2*::*neo*^{R}	pOSCAR-slt2
123V-slt2-c	123V-Δslt2	Δ*slt2*::*neo*^{R}, *slt2*, *hph*	pOSCAR-slt2, slt2, pUCATPH
123V-Δfus3 Δslt2	123V-Δfus3	*fus3*::*hph,* Δ*slt2*::*neo*^{R}	pUCfus3, pOSCAR-slt2
123V-Δste2	123V	Δ*ste2*::*neo*^{R}	pOSCAR-ste2
123V-ste2-c	123V-Δste2	Δ*ste2*::*neo*^{R}, *ste2*, *hph*	pOSCAR-ste2, ste2, pUCATPH
123V-Δfus3 Δste2	123V-Δfus3	*fus3*::*hph,* Δ*ste2*::*neo*^{R}	pUCfus3, pOSCAR-ste2
123V-Δgt1	123V	Δ*gtr1*::*neo*^{R}	pOSCAR-gtr1
123V-gtr1-c	123V-Δgtr1	Δ*gtr1*::*neo*^{R}, *gtr1*, *hph*	pOSCAR-gtr1, gtr1, pUCATPH
123V-Δtsc2	123V	Δ*tsc2*::*hph*	pOSCAR-tsc2
123V-tsc2-c	123V-Δtsc2	Δ*tsc2*::*hph*, *tsc2*, *neo*^{R}	pOSCAR-tsc2, tsc2, pSD1
123V-Δatg1	123V	Δ*atg1*::*hph*	pOSCAR-atg1
123V-atg1-c	123V-Δatg1	Δ*atg1*::*hph*, *atg1*, *neo*^{R}	pOSCAR-atg1, atg1, pSD1

Supplementary Table 2. List of plasmids used in this study.

plasmid	backbone	description	source
pUCATPH	-	*hph*	Lu *et al*., 1994
pSD1	pBluescript II	P_{gpda}, P_{trpc}, neo^R	Nguyen *et al*., 2008
pOSCAR	pPZP-RCS2	*A. tumefaciens* binary vector	Paz *et al*., 2011
pOSCAR-gtr1	pOSCAR	5'H_{gtr1}-neo^R-3'H_{gtr1} (H: 2.0 kb-long homology arms)	This study
pOSCAR-tsc2	pOSCAR	5'H_{tsc2}-*hph*-3'H_{tsc2} (H: 2.0 kb-long homology arms)	This study

Supplementary Table 3. List of DNA oligonucleotides used in this study.

oligo name	sequence (5' to 3')	template (strain or plasmid)	construction/ validation of plasmid/strain
	***gtr1* deletion**		
5flgtr1F 5flgtr1R	GAAACGACAATCTGATCCAAGCTCAAGCTAGTCACCCTCTGCGTGGTAC CAATATCAGTTAACGTCTCGCCATAGTTGACACCGTG	123V	pOSCAR-gtr1
gtr1genF gtr1genR	GTGTCAACTATGGCGAGACGTTAACTGATATTGAAGGAGCAC CTCTTCCCCACAGATAACCCAGGGCTGGTGACGG	pSD1	
3flgtr1F 3flgtr1R	CACCAGCCCTGGGTTATCTGTGGGGAAGAGACGG GCCTGCAGGTCGCGAGCGATCGCGGTACCACCACGAAGATGAAGGATG	123V	
Vdgtr1F Vdgtr1R	CCGCATCTACGTCCTCATCC GGTCCTCGGTCGGGTTGC	123V, 123V-Δgtr1, 123V-gtr1-c	123V-Δgtr1, 123V-gtr1-c
ctrlF ctrlR	GCGCAGTAGGCCAGATCAGG GTCCCGTGCTCGTTTGGTG	123V-Δgtr1	
5flgtr1F 3flgtr1R	GAAACGACAATCTGATCCAAGCTCAAGCTAGTCACCCTCTGCGTGGTAC CAATATCAGTTAACGTCTCGCCATAGTTGACACCGTG	123V	123V-gtr1-c
	***tsc2* deletion**		
5fltsc2F 5fltsc2R	GAAACGACAATCTGATCCAAGCTCAAGCTATTGGCGTCAATCTGCTTGTC CCACTAGCATTACACCGGGACATAGGCTCGTCTG	123V	pOSCAR-tsc2
tsc2-hygF	CGAGCCTATGTCCCGGTGTAATGCTAGTGGAGGTCAAC	pUCATPH	

tsc2-hygR	CAAGGGTGGACTGCGTTGTGTCGCCCTTATTCGAC		
3fltsc2F	GAATAAGGGCGACACAACGCAGTCCACCCTTGTATC	123V	
3fltsc2R	GCCTGCAGGTCGCGAGCGATCGCGGTACAGTATCTGCCTCTTGCCAAC		
Vdtsc2F	CGCCAACCCAGAGGACTTTC	123V, 123V-Δtsc2, 123V-tsc2-c	123V-Δtsc2, 123V-tsc2-c
Vdtsc2R	GTGGCCATTGTGCGACTTG		
ctrlF	GCGCAGTAGGCCAGATCAGG	123V-Δtsc2	
ctrlR	GTCCCGTGCTCGTTTGGTG		
5fltsc2F	GAAACGACAATCTGATCCAAGCTCAAGCTATTGGCGTCAATCTGCTTGTC	123V	123V-tsc2-c
5fltsc2R	CCACTAGCATTACACCGGGACATAGGCTCGTCTG		

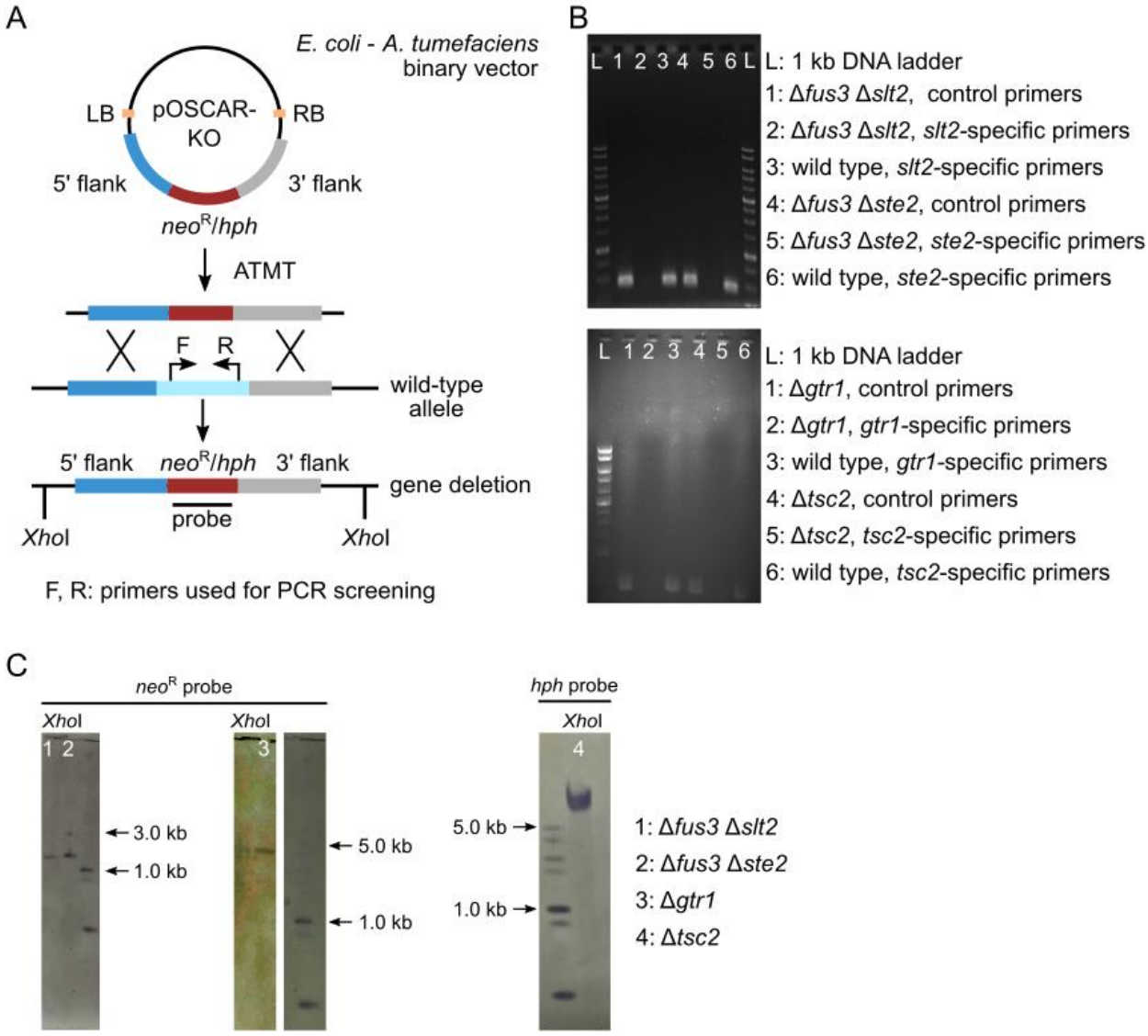

Supplementary Fig. 1. Validation of knockout mutants. **A**. A double homologous recombination-based strategy using *Agrobacterium tumefaciens*-mediated transformation was used for the deletion of the *V. dahliae* 123V homologs of genes *gtr1*, *tsc2*, and the generation of the double knockout mutants Δ*fus3* Δ*slt2* and Δ*fus3* Δ*ste2*. **B**. PCR validation of the deletion mutants Δ*gtr1* and Δ*tsc2* using *gtr1*- or *tsc2*-specific primers as well as the double deletion mutants Δ*fus3* Δ*slt2* and Δ*fus3* Δ*ste2* using *slt2*- or *ste2*-specific primers (Vangalis *et al*., 2021). Primers ctrlF/R (Supplementary Table 3) were used in control reactions for testing template quality. **C**. Validation of mutants by Southern blot after treatment of genomic DNA with *Xho*I, using probes for the *neo*^{R} or the *hph* cassette.

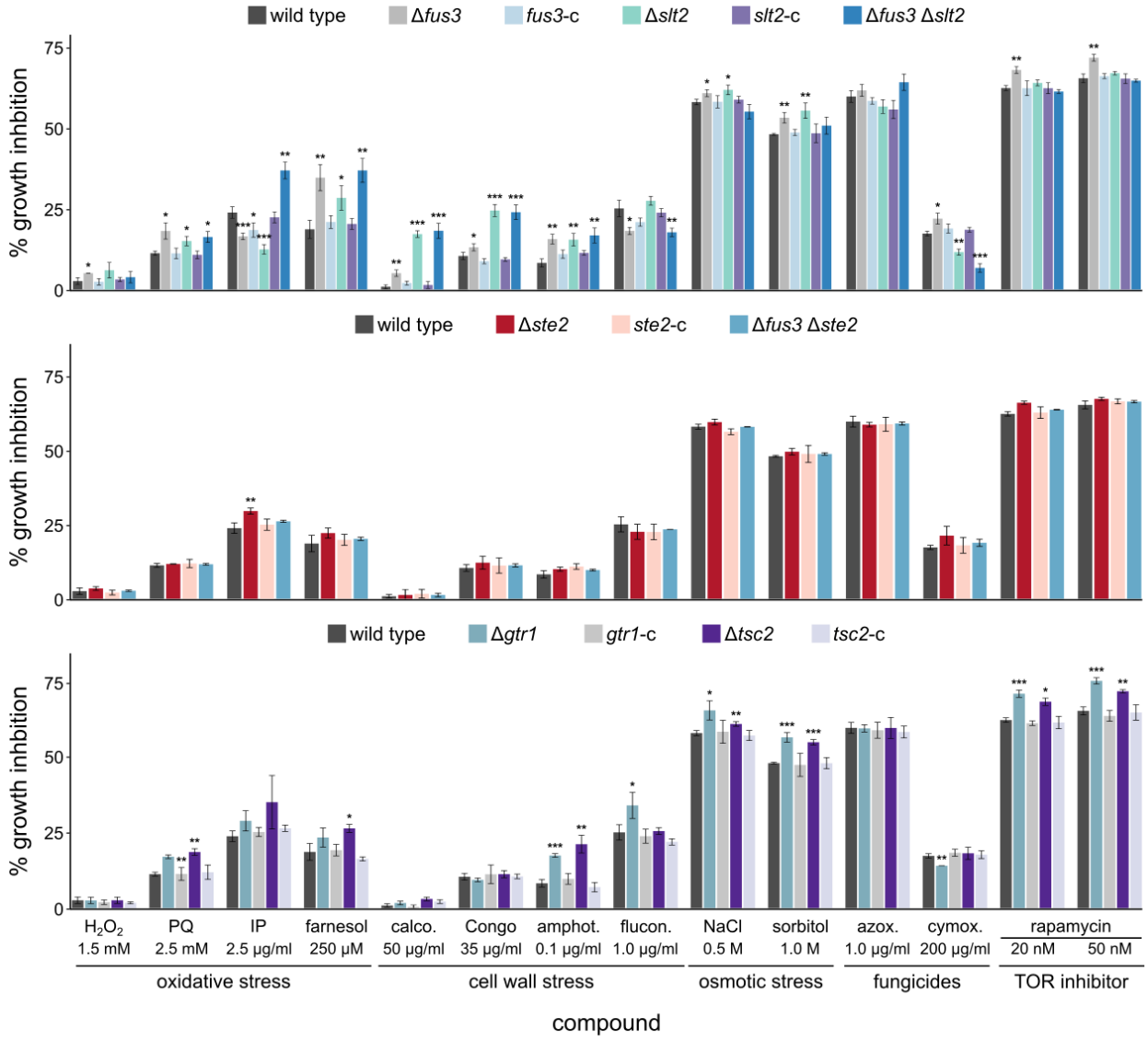

Supplementary Fig. 2. Effect of oxidative and osmotic stresses, cell wall and plasma membrane perturbing agents, and antifungals on the indicated *V. dahliae* strains (**PQ**: paraquat; **azox**: azoxystrobin; **amphot**: amphotericin; **IP**: iprodione; **cymox**: cymoxanil; **calco**: calcofluor white M2R; **Congo**: Congo red; **flucon**: fluconazole). Relative colony growth inhibition was calculated as follows: [(colony diameter on CM − colony diameter in stress condition)/(colony diameter on CM) × 100)]. Bars: SD. Statistical significance of differences to the wild-type strain was calculated by Student's *t*-test (* $p \leq 0.05$, ** $p \leq 0.01$, *** $p \leq 0.001$).

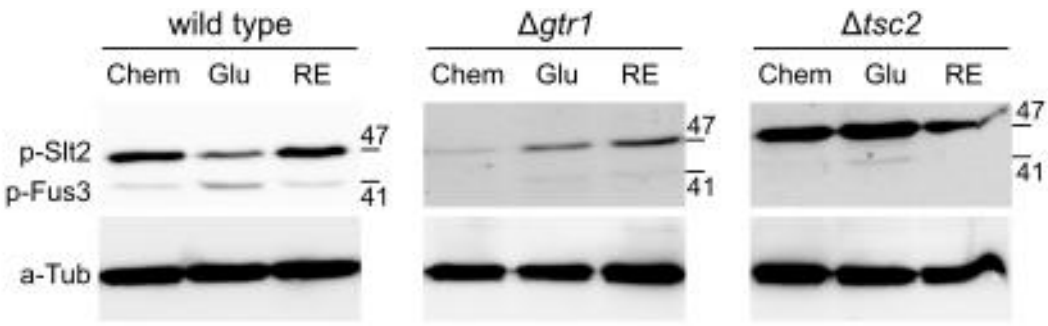

Supplementary Fig. 3. Western blot analysis of Slt2 phosphorylation in the wild-type and the Δ*gtr1* and Δ*tsc2* deletion mutants upon 5 min exposure to glutamate or 10 min exposure to tomato root exudate.

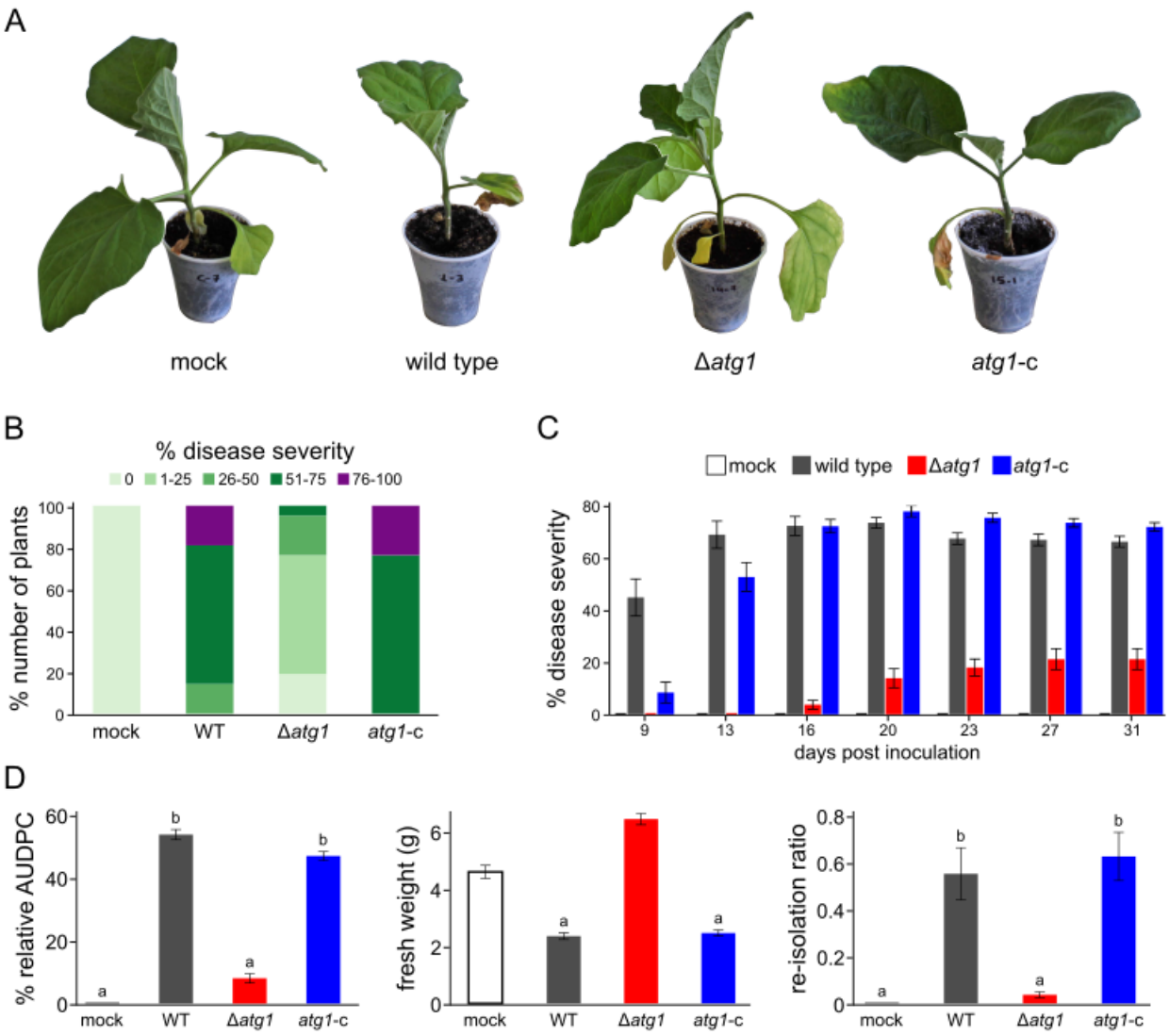

Supplementary Fig. 4. The Δ*atg1* knockout mutant is impaired in pathogenicity. **A**. Representative examples of eggplant plants inoculated with the wild-type strain 123V (WT), the Δ*atg1* deletion mutant and the corresponding complemented strain (*atg1*-c) at 31 days post-inoculation (d.p.i.). **B**. Average disease severity caused by the indicated strains at 31 d.p.i. (21 eggplant seedlings/strain). Non-inoculated plants (mock) served as controls. Percentages in different colours represent different levels of disease severity**. C**. Time-course analysis of disease severity over 31 days. **D**. Average relative AUDPC value of each strain (left), average plant fresh weight (center), and fungal re-isolation ratio at the end of the experiment (31 days). Error bars in **C–D**: SE. Statistical significance of differences between strains was calculated by one-way ANOVA followed by Tukey's post hoc tests. Bars marked with the same letter do not differ significantly ($p \leq 0.05$).